Int. J. Multiphase Flow Vol. 18, No. 3, pp. 353–370, 1992
Printed in Great Britain.

0301-9322/92 $5.00 + 0.00
Pergamon Press Ltd

BEHAVIOR OF MULTIPLE SPHERES IN SHEAR AND POISEUILLE FLOW FIELDS AT LOW REYNOLDS NUMBER

Q. HASSONJEE,† R. PFEFFER and P. GANATOS
The City College of The City University of New York, New York, NY 10031, U.S.A.

(Received 15 November 1990; in revised form 15 October 1991)

Abstract—The multipole truncation technique developed previously by the authors for describing the hydrodynamic interaction of three-dimensional finite clusters of spherical particles at low Reynolds number is used to obtain solutions for the motion of freely suspended particles in planar shear and/or Poiseuille flow fields. Instantaneous configurations containing up to 13 particles are studied and quasi-steady trajectories are obtained for time-varying configurations of two or three particles. Interesting applications of the theory presented in this paper include the time-dependent motion of a chain of spheres with fixed interparticle spacings in shear flow which may serve as a model to study the deformation of a polymer chain and the motion of neutrally buoyant configurations in planar Poiseuille flow to study the lateral migration of particles. The motion of a neutrally buoyant sphere in the presence of a rigidly held sphere in shear flow is also examined. This study reveals a very intriguing behavior in which the free sphere rolls along the fixed sphere but an adverse pressure gradient forces a retrograde motion of its center.

Key Words: particulate Stokes flow, two-phase flow, low Reynolds number hydrodynamics, hydrodynamic interaction of particles, multiple truncation technique

1. INTRODUCTION

Knowledge of the hydrodynamic interaction for multiparticle configurations in shear or Poiseuille flow is essential in predicting the rheological behavior of suspensions. Suspensions provide an economical way of transporting large quantities of solid particulate material in industry such as pulp handling in paper manufacture and petroleum processing in fluidized beds. Self-diffusion of cells in blood is also of great importance. However, as yet, no exact multiparticle hydrodynamic interaction theory exists for shear and Poiseuille flows.

Exact solutions for two spheres in a shear flow are available in the literature. Lin *et al.* (1970) obtained an exact solution of the Stokes equations for the motion of two spheres of arbitrary size and arbitrary orientation with respect to a shear field by using spherical bipolar coordinates. Arp & Mason (1977) presented a general method of calculating forces, torques and translational and rotational velocity components of a pair of equally-sized rigid spheres in a viscous fluid undergoing uniform shear flow. The method is based on the matrix formulation of the hydrodynamic resistances by Brenner & O'Neill (1972).

Far-field interactions for three or more spherical particles have been considered by Mazur & Van Saarloos (1982). These authors developed a general scheme for evaluating the mobility tensor for any three-dimensional configuration of spheres and derived explicit expressions up to order R^{-7}, where R is the interparticle spacing. Their expressions are identical with those previously obtained by Kynch (1959) using the method of reflections. Applications of the theory have been reported by Kamel & Tory (1989) for special planar configurations of sedimenting spheres and by Ladd (1988) for periodic configurations.

Durlofsky *et al.* (1987) developed a very efficient simulation technique, termed the multipole moment method, which permits the rapid evaluation of the force and torque on finite clusters of spherical particles. The method accounts for the many body interactions at large spacings in a manner equivalent to the method of reflections and lubrication forces at close spacings by considering pair interactions. The sphere mobility matrix is first formed by expanding the integral formulation for Stokes flow for a J sphere system in conjunction with Faxen's laws for the particle velocities in the moments of the force distribution on the surface of each particle. The mobility

†Present address: E.I. Dupont Co., Benger Laboratory, Waynesboro, VA 22980, U.S.A.

matrix is inverted to yield a far-field approximation to the resistance matrix. Then lubrication is introduced in a pairwise additive manner using the exact two-body resistance functions calculated by Arp & Mason (1977). Owing to its low computational cost, the method can be used to simulate the time-dependent motion of large systems of particles. However, since only the first few terms in the series expansion for the velocity field are used, the method properly accounts for the multibody interactions when the particle spacing is large and the neglected terms are vanishingly small. Moreover, the method does not readily permit evaluation of the higher order terms, nor does it readily permit evaluation of the fluid velocity field. The method has been applied to study the resuspension of spheres in shear flow in a parallel-walled channel by Durlofsky & Brady (1989).

Tran-Cong & Phan-Thien (1989) have applied the boundary integral technique to treat the hydrodynamic interaction of two spheroidal or three spherical particles at low Reynolds number. The boundary integral method is ideally suited for handling irregularly shaped or deformable bodies. However, for rigid spherical particles it appears advantageous both in terms of accuracy and computational effort to utilize a representation of the disturbance field in terms of a superposition of the fundamental singular solutions of the Stokes equations in spherical coordinates.

Previously we developed (Hassonjee *et al.* 1988) a method of solution, called the multipole truncation technique, for treating three-dimensional clusters of arbitrarily sized spherical particles and accounting for the multiparticle interactions at any given spacing. This study addressed the mobility problem for a multiparticle configuration settling freely under gravity and the resistance problem for clusters of particles fixed in space in a uniform flow field. It did not consider the mobility and resistance problems in shear or Poiseuille flow which is the topic of the present paper.

The multipole truncation technique uses a linear superposition of Lamb's spherical harmonic solution of the creeping flow equations capable of describing an arbitrary disturbance on the surface of a sphere. The unknown constants in the series are determined by a procedure which involves satisfying the no-slip boundary conditions on the surface of each sphere simultaneously for all particles. This is accomplished by expressing the solutions in spherical coordinates in the form of a Fourier series and using the orthogonality property of the eigenfunctions in the azimuthal direction to satisfy the no-slip boundary conditions exactly at discrete rings on the surface of each sphere. The order of truncation of the Fourier series and the number of boundary collocation rings on each sphere determines the number of unknown constants introduced in the superposed series solutions. Using this method any desired degree of accuracy can be obtained by increasing the number of terms in the Fourier series and the number of collocation rings on each sphere. The ability of this method to reproduce exact bipolar solutions for two spheres settling freely under gravity was demonstrated in Hassonjee *et al.* (1988). It was also shown that the method can be used to obtain solutions of multiparticle configurations for as many as 64 spheres fixed in space in a uniform flow and can also easily be used to obtain the fluid velocity field around multiparticle configurations.

The present paper presents a modification of the multipole truncation technique developed in Hassonjee *et al.* (1988) for evaluating the hydrodynamic interactions of clusters of three-dimensional multiparticle configurations in planar shear and/or Poiseuille flow. Section 2 briefly summarizes the salient features of the theory for shear and Poiseuille flow. In section 3 the hydrodynamic interaction of multiparticle configurations in shear flow is examined. In section 4 the lateral migration of particles in Poiseuille flow is considered. Section 5 deals with the time-dependent motion of three linked spheres having fixed interparticle spacings in shear flow. Finally, in section 6, solutions for the motion of a neutrally buoyant sphere in shear flow in the presence of a rigidly held sphere are presented which reveal an unusual behavior in the motion of the neutrally buoyant sphere.

2. FORMULATION FOR SHEAR AND POISEUILLE FLOWS

In this section, the theory developed in Hassonjee *et al.* (1988) for evaluating the hydrodynamic interaction of unrestricted three-dimensional multiparticle configurations in a uniform flow is modified to treat three-dimensional multiparticle configurations suspended freely in a planar shear

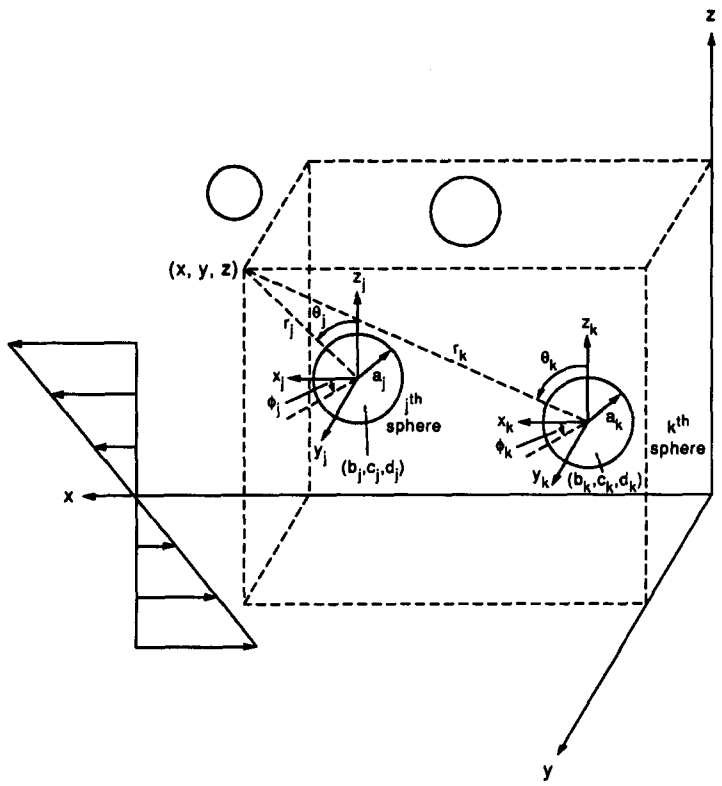

Figure 1. Geometry of system of J spheres suspended in a shear flow.

and/or Poiseuille flow. The reader is referred to Hassonjee *et al.* (1988) for a detailed explanation of the method of solution, since only the key features and modifications of the theory are presented here.

Figure 1 shows the geometry for a cluster of J spheres arranged in an arbitrary three-dimensional configuration in a viscous fluid. The jth and kth spheres in the cluster are centered at the points (b_j, c_j, d_j) and (b_k, c_k, d_k), respectively, in a cartesian global coordinate system (x, y, z). The fluid velocity field in a stationary coordinate system whose origin lies at the center of the kth sphere consists of three parts:

$$\mathbf{V}_k = \mathbf{V}_{k,s} + \mathbf{V}_{k,p} + \mathbf{V}_{k,d}. \qquad [1]$$

Here $\mathbf{V}_{k,s}$ and $\mathbf{V}_{k,p}$ describe planar shear and Poiseuille flow, respectively, which can be expressed in global cartesian coordinates as

$$\mathbf{V}_{k,s} = Sz\mathbf{i} \qquad [2a]$$

and

$$\mathbf{V}_{k,p} = V_c\left[1 - \frac{(z-\eta)^2}{\beta^2}\right]\mathbf{i}, \qquad [2b]$$

where S is the rate of shear and V_c, β and η are the parameters defining the parabolic shape of the Poiseuille flow. Using the coordinate transformations

$$\mathbf{i} = \sin\theta_k \cos\phi_k \hat{e}_{r_k} + \cos\theta_k \cos\phi_k \hat{e}_{\theta_k} - \sin\phi_k \hat{e}_{\phi_k} \qquad [3a]$$

and

$$z = r_k \cos\theta_k + d_k, \qquad [3b]$$

$\mathbf{V}_{k,s}$ and $\mathbf{V}_{k,p}$ are written in terms of spherical coordinates (r_k, θ_k, ϕ_k) originating at the center of the kth sphere as

$$\begin{aligned}\mathbf{V}_{k,s} = & S(r_k \cos\theta_k + d_k) \sin\theta_k \cos\phi_k \hat{e}_{r_k} \\ & + S(r_k \cos\theta_k + d_k) \cos\theta_k \cos\phi_k \hat{e}_{\theta_k} \\ & - S(r_k \cos\theta_k + d_k) \sin\phi_k \hat{e}_{\phi_k}\end{aligned} \quad [4a]$$

and

$$\begin{aligned}\mathbf{V}_{k,p} = & V_c\left[1 - \frac{(r_k \cos\theta_k + d_k - \eta)^2}{\beta^2}\right] \sin\theta_k \cos\phi_k \hat{e}_{r_k} \\ & + V_c\left[1 - \frac{(r_k \cos\theta_k + d_k - \eta)^2}{\beta^2}\right] \cos\theta_k \cos\phi_k \hat{e}_{\theta_k} \\ & - V_c\left[1 - \frac{(r_k \cos\theta_k + d_k - \eta)^2}{\beta^2}\right] \sin\phi_k \hat{e}_{\phi_k}.\end{aligned} \quad [4b]$$

$\mathbf{V}_{k,d}$ in [1] is the fluid velocity disturbance field produced by the J particles which can be represented by a superposition of Lamb's spherical harmonic solution for each particle and is given by

$$\begin{aligned}\mathbf{V}_{k,d} = \sum_{j=1}^{J} \sum_{n=1}^{\infty} \Bigg[& \nabla \times (\mathbf{r}_j \chi_{-(n+1),j}) + \nabla \Phi_{-(n+1),j} \\ & - \frac{(n-2)}{\mu 2n(2n-1)} r_j^2 \nabla P_{-(n+1),j} + \frac{(n+1)}{\mu n(2n-1)} \mathbf{r}_j P_{-(n+1),j} \Bigg],\end{aligned} \quad [5]$$

where χ, Φ and P are solid spherical harmonic functions given by

$$\begin{bmatrix} \chi_{-(n+1),j} \\ \Phi_{-(n+1),j} \\ P_{-(n+1),j} \end{bmatrix} = \sum_{m=0}^{n} P_n^m(\zeta_j) \frac{1}{r_j^{n+1}} \left\{ \begin{bmatrix} A_{jmn} \\ C_{jmn} \\ E_{jmn} \end{bmatrix} \cos m\phi_j + \begin{bmatrix} B_{jmn} \\ D_{jmn} \\ F_{jmn} \end{bmatrix} \sin m\phi_j \right\}. \quad [6]$$

Here (r_j, θ_j, ϕ_j) are spherical coordinates whose origin coincides with the center of the jth sphere, $\zeta_j = \cos\theta_j$, P_n^m is the associated Legendre polynomial and $A_{jmn} - F_{jmn}$ are unknown constants which are determined by satisfying the no-slip boundary conditions on the surface of each sphere. The solution procedure for determining these constants follows along the same lines as that described in Hassonjee *et al.* (1988) with the exception of the additional terms introduced by the free stream solution [4a,b]. The coordinates of the jth sphere are first written in terms of a single spherical coordinate system whose origin lies at the center of the kth sphere. Since the associated Legendre function P_n^m is zero for $m > n$, one can replace the summations $\Sigma_{n=1}^{\infty} \Sigma_{m=0}^{n}$ in [5] and [6] by $\Sigma_{m=0}^{\infty} \Sigma_{n=m(n\neq 0)}^{\infty}$ without any loss of terms and the term $j = k$ is extracted from the outer summation in j. This manipulation reveals that the eigenfunctions in ϕ_k constitute a complete Fourier series whose orthogonality properties can be used to satisfy the no-slip boundary conditions on any azimuthal ring, θ_k = constant, on the surface of the kth sphere. The integrations involved in the inversion of this Fourier series are performed numerically with the exception of the terms in the free stream velocity which may easily be performed analytically. The final expressions are given in the appendix.

For the resistance problem in which the $6J$ translational and angular velocity components are prescribed and one wishes to determine the forces and torques on each sphere, the two infinite series in n and m in [A.1]–[A.12] are truncated after N and M terms, respectively, yielding $6JMN$ unknown constants. However, when $m = 0$ the coefficients of the constants B_{j0n}, D_{j0n} and F_{j0n} are identically zero for all three velocity components. Thus, one needs only $3JN(2M - 1)$ independent equations which are provided by [A.1]–[A.12].

The hydrodynamic force and torque acting on the jth particle may easily be obtained from expressions found in Happel & Brenner (1973, p. 67) and are given by

$$\mathbf{F}_j = -4\pi\nabla(r_j^3 P_{-2}) = -4\pi[E_{j11}\mathbf{i} + F_{j11}\mathbf{j} + E_{j01}\mathbf{k}] \quad [7a]$$

and

$$\mathbf{T}_j = -8\pi\mu\nabla(r_j^3 \chi_{-2}) = -8\pi\mu[A_{j11}\mathbf{i} + B_{j11}\mathbf{j} + A_{j01}\mathbf{k}]. \quad [7b]$$

We now consider the mobility problem, in which the force and torque acting on each particle is prescribed, and we seek to determine the resulting translational and angular velocities. To illustrate, we examine the special case of a neutrally buoyant finite cluster of spheres suspended in an unbounded media. Equating the force and torque acting on each particle to zero yields:

$$E_{j11} = F_{j11} = E_{j01} = 0 \quad [8a]$$

and

$$A_{j11} = B_{j11} = A_{j01} = 0. \quad [8b]$$

The $6J$ unknown particle translational and angular velocity components contained in [A.1]–[A.12] are exactly equal in number to the $6J$ constants evaluated in [8a,b]. Therefore, the total number of unknowns remains the same.

In Hassonjee *et al.* (1988) the accuracy and convergence characteristics of the solution procedure were examined in detail. The ability of this technique to reproduce exact solutions for two spheres settling freely under gravity at different interparticle spacings and orientations was demonstrated. We have also been able to reproduce the exact solutions of Lin *et al.* (1970) for the translational and angular velocities of two neutrally buoyant spheres in shear flow for center-to-center spacings >1.1 particle diameters. Although the theory is valid at closer spacings, the series become slowly convergent making the procedure computationally prohibitive. Thus, in this paper we have restricted our attention to center-to-center spacings $R/2a \geqslant 1.1$, unless otherwise noted. Numerical tests show that convergence to within three or four significant figures can be achieved at a center-to-center spacing of 1.12 particle diameters using 8 rings on each sphere and retaining 6 terms in the Fourier series. At a spacing of 1.54 diameters, only 6 rings on each sphere and 5 terms in the Fourier series were required to achieve the same accuracy. Tables containing the results of these convergence tests may be found in Hassonjee (1987).

3. HYDRODYNAMIC INTERACTION OF SPHERES IN A SHEAR FLOW

In this section we consider the hydrodynamic interaction of clusters of neutrally buoyant spheres in shear flow and demonstrate the importance of accounting for the interaction among all particles in the configuration. Failure of theories based on piecewise additivity assumptions are highlighted with some simple examples. It is worth pointing out that such failures may be anticipated on the basis of symmetry arguments that may be found in Brenner's (1964) work on the subject.

Consider two identical unconstrained neutrally buoyant spheres at a center-to-center spacing of 4 radii lying in the plane of shear ($y = 0$) at an angle of 30° with respect to the x-axis, as shown in figure 2(a). Both spheres have positive x- and z-velocity components and, from symmetry, the y-component of the velocity of both spheres is obviously zero. The velocity components of the sphere at the origin are shown in figure 2(a). Next consider two spheres in the plane $z = 0$ with the line joining the centers of the two spheres making an angle of 30° with respect to the x-axis, as shown in figure 2(b). The x- and y-velocity components of both spheres are zero and, in particular, the sphere at the origin has a positive z-velocity component as shown in the figure. Next we look at a three-sphere configuration where the first sphere is placed at the origin, the second sphere is in the plane of shear ($y = 0$) and the third sphere lies in the plane $z = 0$. The line joining the centers of spheres 2 and 1 and spheres 3 and 1 makes an angle of 30° with respect to the x-axis,

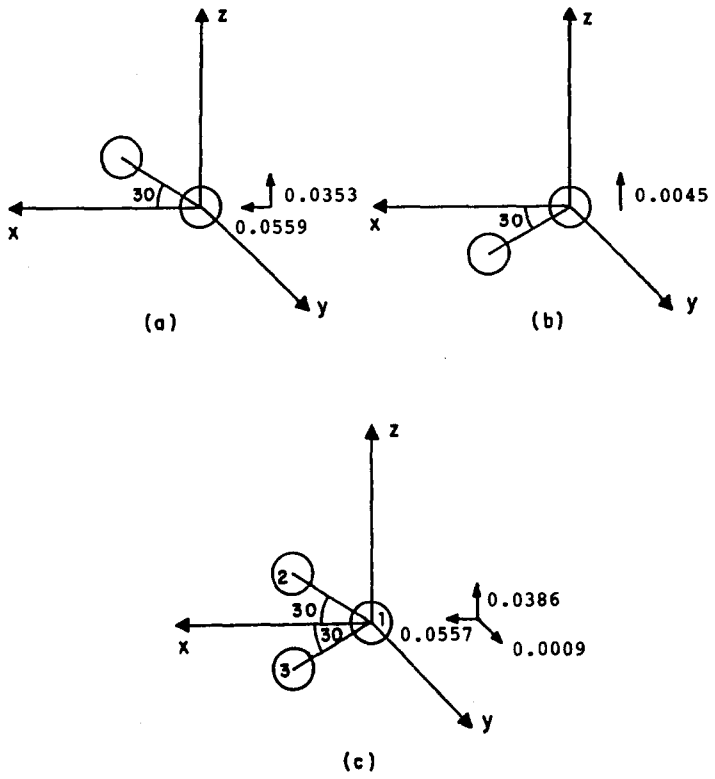

Figure 2. (a) Two spheres in the plane $y = 0$ with their line of centers inclined at 30° with respect to the x-axis. (b) Two spheres in the plane $z = 0$ with their line of centers oriented at 30° with respect to the x-axis. (c) Three-sphere configuration, where spheres 1 and 2 are in the plane $y = 0$ with their line of centers inclined at 30° with respect to the x-axis and spheres 1 and 3 are in the plane $z = 0$ with their line of centers oriented at 30° with respect to the x-axis. Center-to-center spacing between all spheres and the sphere at the origin is 4 radii. All velocities are nondimensionalized by aS.

as shown in figure 2(c), and the center-to-center spacing between the sphere at the origin and the other two spheres is 4 radii. This configuration of three spheres is a combination of the earlier two-sphere configurations. Note that if the velocity components of the sphere at the origin for the configurations shown in figures 2(a) and 2(b) are simply added, the sum is remarkably close to the value of the velocity components of the sphere at the origin for the configuration shown in figure 2(c). However, this simple superposition fails to predict a nonzero y-translational velocity component of the sphere at the origin for the three-sphere configuration shown in figure 2(c) which the present solution shows has a value of $0.0009aS$. This example shows that using paired interactions to describe multiple particle behavior can miss an effect which arises from the simultaneous three-body interactions.

A similar behavior is also observed in a four-body interaction. When three unconstrained neutrally buoyant spheres are placed at the corners of a right triangle in the plane of shear, as shown in figure 3(a), all three spheres have nonzero x- and z-velocity components and, in particular, for a center-to-center spacing along the x- and z-axes of 4 particle radii, the sphere at the origin has the positive x- and z-velocity components shown. Next, for three spheres placed at the corners of a right triangle in the plane $x = 0$, as shown in figure 3(b), all three spheres have only an x-velocity component. The velocity of the sphere at the origin for an interparticle spacing along the y- and z-axes of 4 radii is reported in the figure. Finally, for three spheres placed at the corners of a right triangle in the plane $z = 0$, as shown in figure 3(c), all three spheres have only a z-velocity component. The velocity of the sphere at the origin for a center-to-center spacing along the x- and y-axes of 4 radii is shown in the figure. Now for a four-sphere configuration, which is a combination of the previous three sphere configurations shown in figure 3(d), the sphere at the origin should not have a y-translational velocity component according to the three-body interactions. However, the present solution shows a nonvanishing y-velocity component for the sphere at the origin in this four-sphere configuration. At a center-to-center spacing of 4 radii between the sphere at the origin

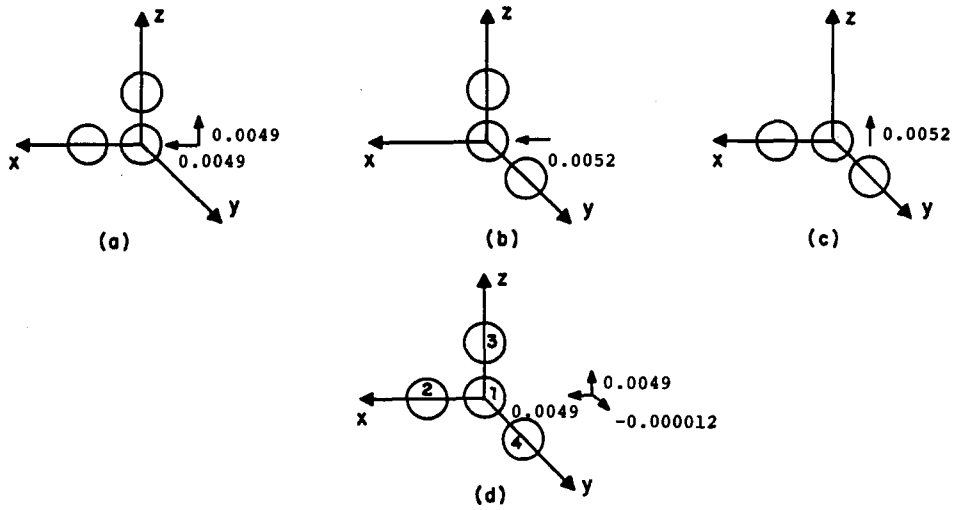

Figure 3. (a) Three spheres in the plane $y = 0$ at the vertices of a right triangle. (b) Three spheres in the plane $x = 0$ at the vertices of a right triangle. (c) Three spheres in the plane $z = 0$ at the vertices of a right triangle. (d) Four-sphere configuration, where sphere 1 is placed at the origin and spheres 2, 3 and 4 are placed on the axes. Center-to-center spacing between all spheres and the sphere at the origin is 4 radii. All velocities are nondimensionalized by aS.

and the other spheres, the value of this velocity component is $-0.000012aS$.† This example demonstrates the fact that even three-body interactions cannot always predict the behavior of a four-sphere configuration and underscores the importance of treating the multiparticle interactions simultaneously.

In this section, all calculations were performed with $N = 6$ and $M = 5$. Convergence was checked by redoing the calculations with $N = 8$ and $M = 6$. The values of the velocities reported in figures 2 and 3 are converged to the number of digits shown.

Leighton & Acrivos (1987) observed a shear-induced migration of particles in concentrated suspensions. In a three-dimensional multiparticle suspension, spheres experience a self-diffusion perpendicular to the plane of shear. While a rigorous theoretical demonstration of the phenomenon would require three-dimensional time-dependent calculations showing a clear migration of particles normal to the plane of shear, the induced motion of the sphere at the origin in the two examples considered above may be an indication of this effect.

4. MIGRATION OF NEUTRALLY BUOYANT SPHERES IN A PLANAR PARABOLIC FLOW

In this section we present a study of the migration of clusters of neutrally buoyant spheres in a planar Poiseuille flow. Drift from regions of high shear rate to low shear rate has been predicted theoretically for purely hydrodynamic interactions by Koch (1989) and for irreversible interactions in concentrated suspensions by Leighton & Acrivos (1987).

Figure 4 shows a planar configuration of 13 identical neutrally buoyant spheres placed in a parabolic flow. Sphere 1 is located at the center of two concentric regular hexagons. Spheres 2–13 are located at the corners of the two hexagons. This arrangement produces a planar triangular array with a center-to-center spacing of 1.68 (approx.) diameters between adjacent spheres. The concentration of the triangular unit cell is 0.325 in the plane of the sphere centers. All of the spheres are free to translate and rotate. The free stream flow has a planar parabolic profile given by

$$V_p = V_c\left[1 - \frac{(z-\eta)^2}{\beta^2}\right], \qquad [9]$$

†The very small magnitude of this value may raise a question as to its validity. Convergence tests show that for $N = 4$ and $M = 3$ the value is -0.000017, for $N = 6$ and $M = 4$ it is -0.0000121 and for $N = 8$ and $M = 6$ it is -0.0000121. Thus, the value appears to have converged to three significant figures.

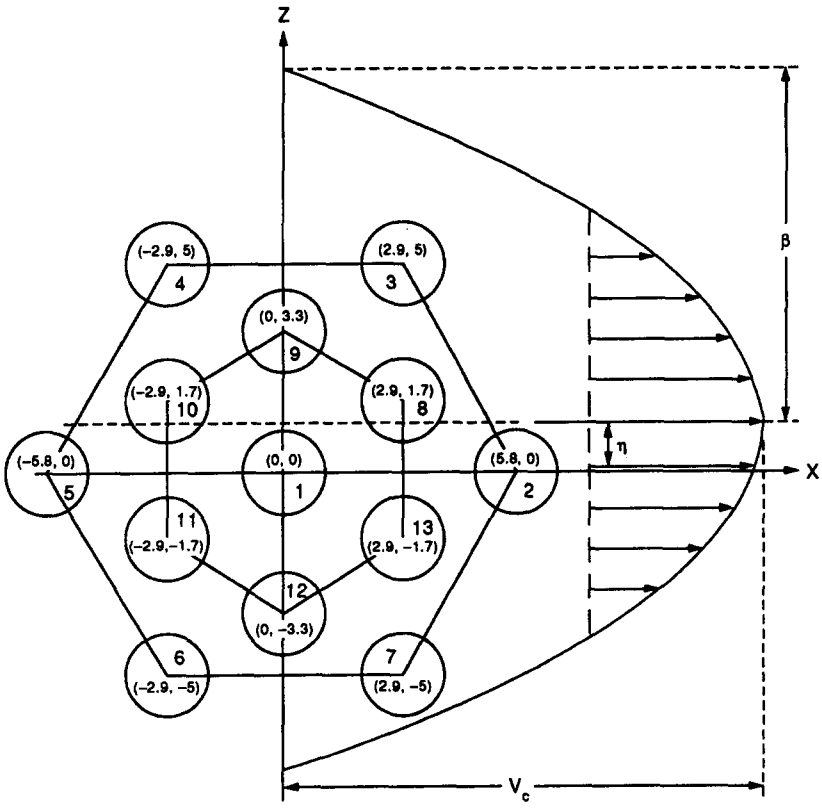

Figure 4. Schematic of the multiparticle configuration of 13 neutrally buoyant spheres placed in a planar parabolic profile defined by the expression $V_c[1 - ((z - \eta)^2/\beta^2)]$. Sphere 1 is at the center of two concentric hexagons. Spheres 2–7 are placed at the corners of the outer hexagon and spheres 8–13 are placed at the corners of the inner hexagon. The coordinates of the sphere centers are nondimensionalized by the sphere radius.

where, as shown in figure 4, β is the distance from the centerline where the free stream velocity vanishes and η is the displacement of the centerline from the center of the multiparticle configuration. For all problems under consideration in this section, the centerline velocity was normalized to unity and β was taken to be 20 sphere radii. We used $N = 4$ and $M = 3$ in all numerical calculations.

Numerous runs were done with this instantaneous configuration of 13 spheres where the parameter η was varied while keeping the parameter β constant. Figure 5 shows the lateral drift velocity W_j (z-component of velocity) of the jth particle as a function of η. Owing to symmetry, spheres 1, 9 and 12 do not drift laterally. For $\eta = 0$, the center of the configuration coincides with the centerline of the two-dimensional Poiseuille profile and owing to symmetry, spheres 2 and 5 also do not drift laterally. The remaining leading spheres tend to drift away from the plane of symmetry ($z = 0$) from a region of low shear to a region of high shear flow, while just the opposite is true for the trailing spheres. For $\eta \geqslant 6$ (see figure 4) the entire configuration lies below the centerline of the Poiseuille profile. In this range of η, figure 5 shows that all of the leading spheres drift from a region of low shear to high shear flow while all the trailing spheres drift from the high to low shear region. The drift of the overall system of particles from regions of high shear to low shear flow over a period of time is not immediately evident from examination of the particle velocities at one instant of time.

Although possible in principle, the computation time which would be required to do a 13-sphere time-dependent simulation by the present method of solution is prohibitive. However, many of the features of the motion of neutrally buoyant particles in Poiseuille flow may be realized in a time-dependent simulation involving three particles. Such a run is shown in figure 6. In this figure, time t has been nondimensionalized by a/V_c. At $t = 0$, the spheres are placed at the corners of an equilateral triangle at a center-to-center spacing of 4 radii, with sphere 1 at a distance of 4 radii

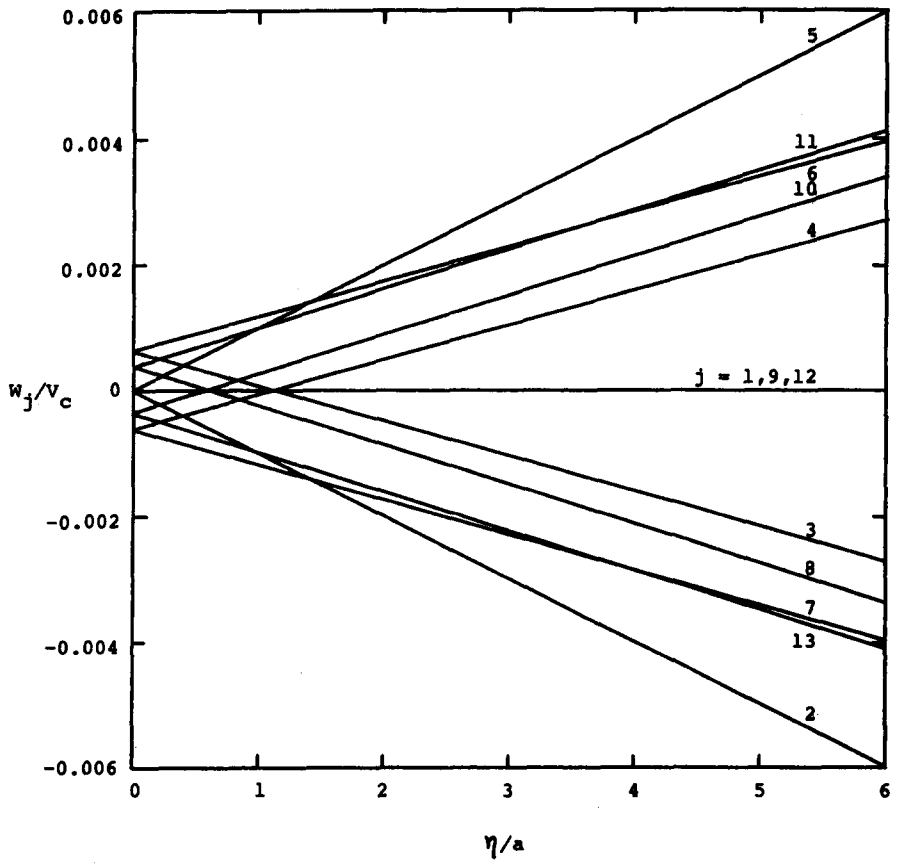

Figure 5. Lateral drift velocity of the 13 particles in the configuration shown in figure 4.

from the plane of zero shear which is denoted by the x-axis. The flow is directed to the right. At this instant in time the leading spheres are moving away from the plane of zero shear while the trailing sphere is moving towards it. This behavior is consistent with that previously observed for

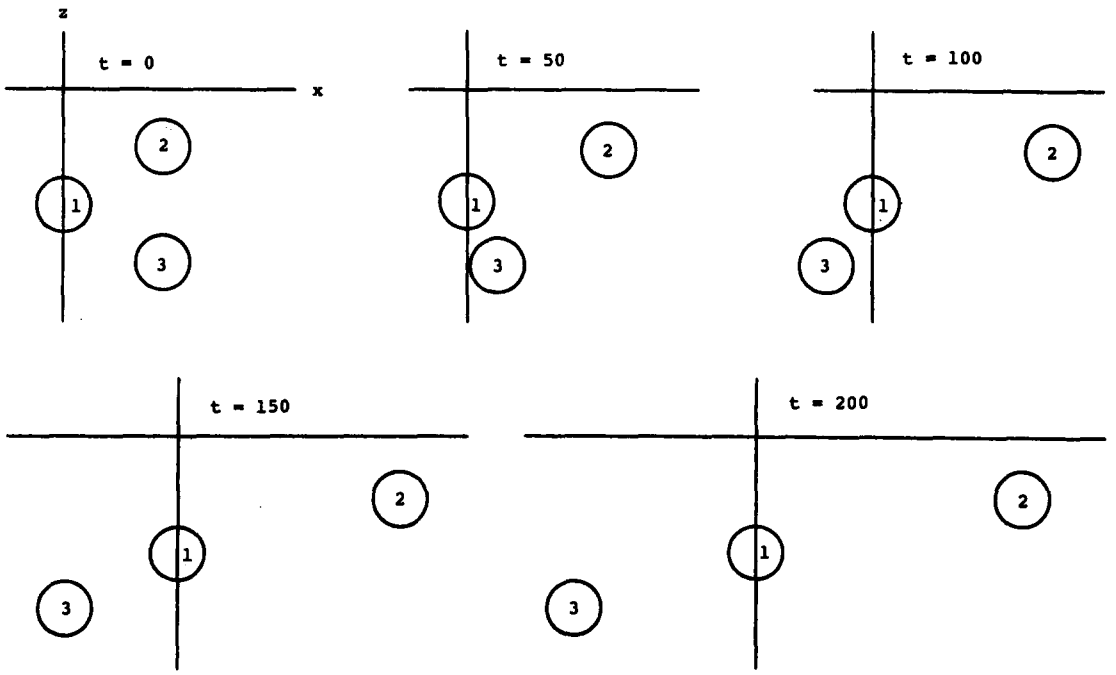

Figure 6. Time-dependent run of three neutrally buoyant spheres originally in an equilateral triangular configuration in a planar parabolic flow.

the 13-sphere configuration. Subsequent frames are shown in a coordinate system which is translating to the right to follow the center of sphere 1. As expected, sphere 2 which is closest to the centerline travels the fastest, while sphere 3 which is furthest away travels the slowest. As sphere 3 swings by sphere 1, it causes sphere 1 to move slightly upward but then moves back down as sphere 3 moves away. The center of mass of the configuration in the lateral direction remains very nearly constant for all time. For the configuration considered, the spheres tend to align themselves in a straight line passing through the center of mass of the configuration parallel to the direction of flow. If a large number of randomly dispersed spheres were present, statistically there would be an equal number of particles on each side of the plane of zero shear and thus the center of mass of the configuration would have to coincide with the plane of zero shear. Therefore, over a period of time, as the particles drift laterally toward the center of mass of the configuration, they would appear to migrate from a region of high shear to a region of low shear flow.

5. TIME-DEPENDENT MOTION OF A CHAIN OF SPHERES WITH FIXED INTERPARTICLE SPACINGS

In polymer science it is very useful to know the deformation of a polymer chain in shear flow to determine the properties of a particular polymer. The application of this theory to practical problems is demonstrated by studying the deformation of a chain of three spheres with fixed interparticle spacings in shear flow.

Consider three identical spheres placed in the plane of shear. The hydrodynamic interaction among the three particles can easily be determined by the theory presented in section 2. However, the theory must be modified to include the constraint of fixed interparticle spacings, which would be present if the spheres were somehow linked such as by thin rigid rods. The required modifications are outlined below.

Figure 7 shows a schematic of three spheres in a plane. R_{12} and R_{23} are the fixed interparticle spacings between spheres 1 and 2 and spheres 2 and 3, respectively, and it is required that these spacings remain constant. U_j and W_j are the x- and z-velocity components of the jth sphere, respectively. F_{12} and F_{23} are the tensile forces transmitted through the rods joining the centers of spheres 1 and 2 and spheres 2 and 3. We assume that the particles are free to rotate so the condition of zero torque on each sphere given by [8b] is still valid. However, the hydrodynamic force acting on each particle does not vanish due to the additional force exerted on that particle through the rods. Therefore, condition [8a] is no longer valid and this increases the number of unknowns by $3J$ since E_{j11}, E_{j01} and F_{j11} are no longer zero. For our particular case of three spheres in a plane, this introduces six additional unknowns corresponding to E_{j11} and E_{j01} for $j = 1, 2, 3$ as F_{j11} is omitted in the planar case. Now an additional six equations are required in order to be able to solve for the unknowns. These are obtained as follows.

In order that the interparticle spacing between spheres 1 and 2 be fixed we must first satisfy the kinematic condition that the translational velocity component of sphere 1 relative to sphere 2 parallel to the line joining their centers must be zero. If the line joining the centers of spheres 1 and 2 makes an angle θ_{12} with respect to the x-axis, then

$$(U_1 - U_2)\cos\theta_{12} + (W_1 - W_2)\sin\theta_{12} = 0. \qquad [10]$$

The kinematic condition for keeping the interparticle spacing between spheres 2 and 3 fixed requires

$$(U_2 - U_3)\cos\theta_{23} + (W_2 - W_3)\sin\theta_{23} = 0, \qquad [11]$$

where θ_{23} is the angle of inclination of the line joining spheres 2 and 3 with the x-axis. Equations [10] and [11] are the first two of the six equations needed for closure.

Next, for quasi-steady motion, we must satisfy the dynamic condition that the sum of the hydrodynamic force and the force exerted by the rod(s) on each particle must be zero. This requirement gives rise to the following additional equations:

$$F_{x_1} - F_{12}\cos\theta_{12} = 0, \qquad [12]$$

$$F_{z_1} - F_{12}\sin\theta_{12} = 0, \qquad [13]$$

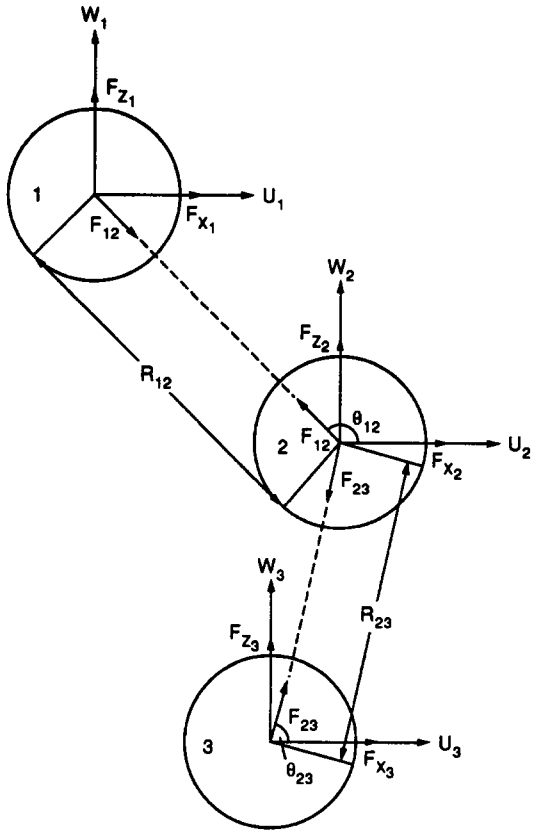

Figure 7. Schematic of a chain of three linked spheres in a plane.

$$F_{x_2} + F_{12}\cos\theta_{12} - F_{23}\cos\theta_{23} = 0, \quad [14]$$

$$F_{z_2} + F_{12}\sin\theta_{12} - F_{23}\sin\theta_{23} = 0, \quad [15]$$

$$F_{x_3} + F_{23}\cos\theta_{23} = 0 \quad [16]$$

and

$$F_{z_3} + F_{23}\sin\theta_{23} = 0, \quad [17]$$

where the hydrodynamic forces F_{x_j} and F_{z_j} can be expressed in terms of the coefficients E_{j11} and E_{j01} using [7a]. This set of six equations [12]–[17] contains two additional unknowns, F_{12} and F_{23}, which can be eliminated to provide the four additional equations needed for closure.

After making the necessary modifications to the general theory, convergence tests were performed for the case of three spheres where the interparticle spacing between spheres 1 and 2 and spheres 2 and 3 were 4 radii and θ_{12} and θ_{23} were 160° and 20°, respectively (see figure 8 for $t = 0$). Table 1 shows the convergence tests for an increasing number of collocation rings N and terms retained in the Fourier series M. The instantaneous x-velocity component of sphere 2 is zero, the x-velocity components of spheres 1 and 3 are equal in magnitude but opposite in sign and the z-velocity and rotational velocity components of spheres 1 and 3 are equal in magnitude and sign. The results for this configuration of three linked spheres in a chain were found to converge somewhat faster than for the general case of three freely moving spheres at the same spacing.

Using a fifth-order Runge–Kutta procedure, time-dependent runs were performed for various initial configurations of three spheres. Figure 8 shows the time-dependent motion of one particular initial configuration. The three spheres were initially placed in a V-shaped configuration in the plane of shear ($y = 0$). The center-to-center distance between spheres 1 and 2 and spheres 2 and 3 was maintained at 4 radii. Spheres 1 and 3 were placed symmetrically about the x-axis at an angle of 20° between each of the links and the x-axis. The time t in figure 8 is nondimensionalized by the shear rate S introduced in [2a]. Subsequent frames show that the configuration gradually opens

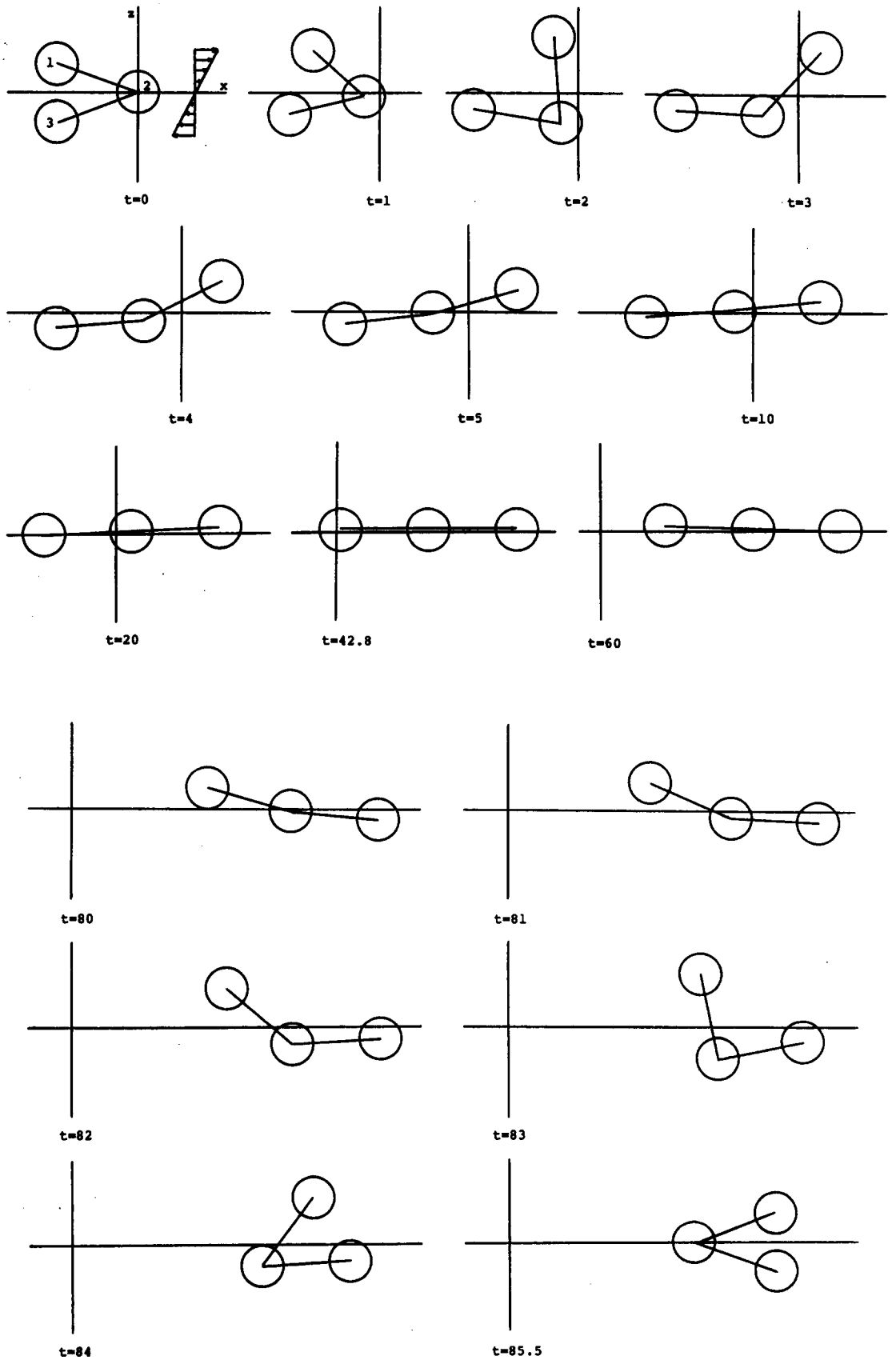

Figure 8. Time-dependent motion of three linked spheres in shear flow.

Table 1. Velocities of three identical neutrally buoyant spheres of radius a connected by thin rods in a chain in shear flow at an orientation where $\theta_{12} = 160°$, $\theta_{23} = 20°$ and $R_{12} = R_{23} = 4a$

N	M	$U_1 = -U_3$	$W_1 = W_3$	$\Omega_{y_1} = \Omega_{y_3}$	$-W_2$	Ω_{y_2}
2	2	0.41133	0.49959	0.92150	0.63053	0.94330
2	3	0.41154	0.49989	0.92172	0.63082	0.94330
2	4	0.41156	0.49990	0.92172	0.63086	0.94326
2	5	0.41157	0.49990	0.92172	0.63086	0.94326
2	6	0.41157	0.49990	0.92172	0.63086	0.94326
4	2	0.42741	0.51759	0.89696	0.65672	0.94548
4	3	0.42755	0.51786	0.89730	0.65683	0.94538
4	4	0.42757	0.51788	0.89730	0.65685	0.94538
4	5	0.42757	0.51788	0.89730	0.65685	0.94538
6	2	0.42814	0.51866	0.89324	0.65764	0.94588
6	3	0.42827	0.51892	0.89354	0.65775	0.94580
6	4	0.42829	0.51894	0.89354	0.65777	0.94578
6	5	0.42829	0.51894	0.89354	0.65777	0.94578
8	2	0.42821	0.51873	0.89290	0.65777	0.94588
8	3	0.42835	0.51900	0.89320	0.65788	0.94580
8	4	0.42836	0.51901	0.89322	0.65790	0.94580
8	5	0.42836	0.51901	0.89322	0.65790	0.94580

N is the number of rings on each sphere, M is the number of eigenfunctions retained in the azimuthal direction. U, V, W and Ω_x, Ω_y, Ω_z are the translational and angular velocity components nondimensionalized by aS and $(1/2)S$, respectively.

up and at $t = 42.8$ forms a straight line parallel to the direction of flow. Continuation of the run shows that at $t = 85.5$, a V-shaped configuration is again formed which, owing to the reversibility of Stokes flow, is congruent to the configuration at $t = 0$. At $t = 171$ the spheres would return to their original positions (at $t = 0$) and the cycle would again be repeated.

For the run shown in figure 8 we used four boundary collocation rings and retained the first three terms of the Fourier series. The maximum deviation in the velocity components between the converged results and the results obtained using four rings and three terms of the Fourier series was 0.2% (see table 1) for the extreme case when spheres 1 and 3 were the closest (interparticle gap of 0.35 diameters).

A similar procedure may be followed to treat more than three particles. The particles may be of unequal size and other types of constraints may be specified between the particles to obtain a more realistic representation of a polymer chain.

6. MOTION OF A NEUTRALLY BUOYANT SPHERE IN THE PRESENCE OF A FIXED SPHERE IN SHEAR FLOW

Consider the two spheres shown in figure 9 at a center-to-center spacing of 4 radii. The line joining the centers of the two spheres is parallel to the direction of flow and lies in the plane where the free stream velocity is zero. When both spheres are neutrally buoyant [see figure 9(a)], the sphere on the left (i.e. sphere 1) moves upward while the sphere on the right (i.e. sphere 2) moves downward with the same magnitude. Both spheres rotate clockwise and there is no net transfer of fluid through the gap between the two spheres. Now suppose that sphere 1 is fixed (translational and rotational velocities prescribed as zero) while sphere 2 is still neutrally buoyant [see figure 9(b)], then sphere 2 continues to rotate in a clockwise direction but translates upward! This is contrary to one's intuition since one would expect that as the free sphere rolls against the fixed sphere, its center should translate downward.

To understand this unusual behavior we consider shear flow past a rigidly held sphere in the absence of the free sphere. If the free sphere were sufficiently small its center would essentially follow the streamline of the flow. The velocity field may readily be derived from Lamb's spherical harmonic solution ([5]) and its cartesian components are given by

$$u = Sz - \frac{Sza^3}{2r^3}\left[1 + 5\frac{x^2}{r^2} + \frac{a^2}{r^2} - 5\frac{a^2x^2}{r^4}\right], \qquad [18a]$$

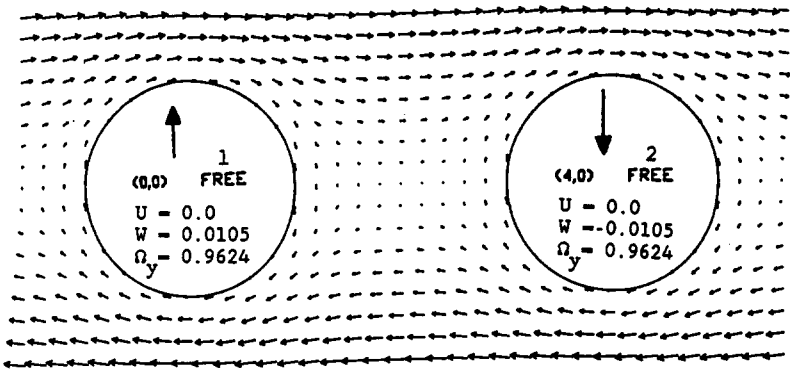

(a)

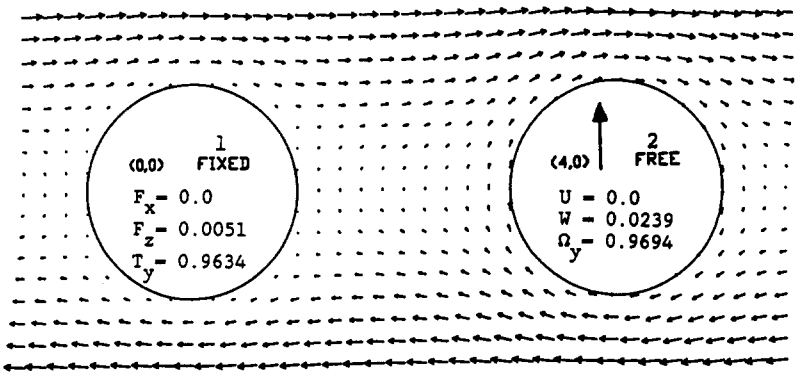

(b)

Figure 9. Fluid velocity field in the vicinity of two identical spheres at a center-to-center spacing of 4 radii in a simple shear flow. Translational and angular velocities are nondimensionalized by aS and $(1/2)S$, respectively. The forces and torques exerted by the fluid on the fixed sphere are nondimensionalized by $6\pi\mu a^2 S$ and $8\pi\mu a^2(1/2)aS$, respectively. (a) Spheres 1 and 2 are neutrally buoyant and free to move. (b) Sphere 1 is fixed and sphere 2 is neutrally buoyant and free to move.

$$v = -\frac{5Sxyza^3}{2r^3}\left[1 - \frac{a^2}{r^2}\right] \qquad [18b]$$

and

$$w = \frac{Sxa^3}{2r^3}\left[1 - 5\frac{z^2}{r^2} - \frac{a^2}{r^2} + 5\frac{a^2z^2}{r^4}\right]. \qquad [18c]$$

The corresponding pressure field is

$$P = P_\infty - 5S\mu\frac{a^3}{r^5}xz, \qquad [19]$$

where the origin of the cartesian coordinate system lies at the center of the fixed sphere and the leading terms in [18a] and [19] represent the far-field shear flow. The velocity field computed from [18a–c] in the plane $y = 0$ is shown in figure 10. We find that even though the net flow across the plane $z = 0$ is zero as required by continuity, the local fluid velocity normal to this plane does not vanish. This may easily be verified by substituting $z = 0$ in [18c], which shows that the fluid moves upward on the right of the sphere and downward on its left. This vertically directed flow is induced by the pressure field (see [19]). As the fluid approaches the fixed sphere from the right it is obstructed by the fixed sphere, resulting in a rise in pressure on the right of the fixed sphere in the region $z < 0$. Similarly, as fluid is withdrawn from the right in the region $z > 0$, it creates a pressure drop. The

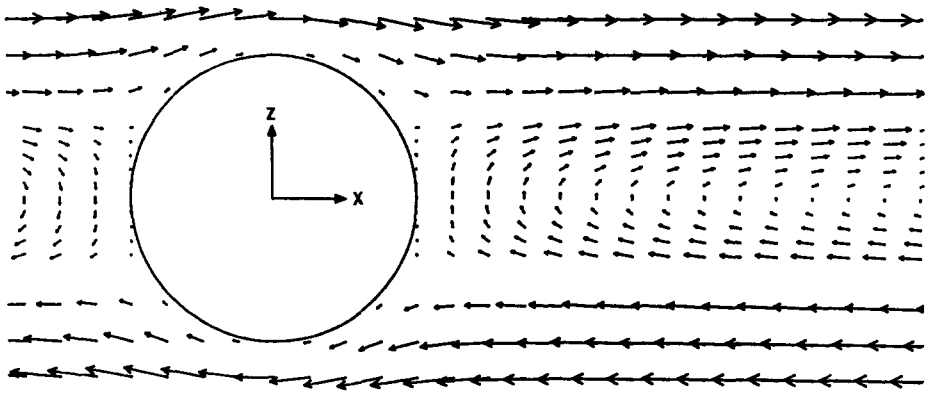

Figure 10. Fluid velocity field in the vicinity of a rigidly held sphere in simple shear flow.

result is an induced flow from the high-pressure to the low-pressure regions shown in figure 10 or an upward velocity of the neutrally buoyant sphere shown in figure 9(b).

Figure 11 shows the z-velocity component of the neutrally buoyant sphere W as a function of interparticle spacing. Actually, W is the total translational velocity of the sphere since for $z = 0$, the x- and y-components are both zero. For large spacings W is positive as explained above. As the spheres are brought closer together, W reaches a maximum at a spacing R/a close to 3. The value of W then drops to zero at $R/a = 2.18$ before becoming negative at closer spacings as the free sphere tends to roll along the fixed sphere. At the critical point in the plane $z = 0$ where W vanishes, the neutrally buoyant sphere is held captive by the fixed sphere, i.e. it rotates in a clockwise direction without translation. W must take a minimum value somewhere in the range $2 \leqslant R/a \leqslant 2.18$ since we must have $W = 0$ as $R/a \to 2$ (i.e. at contact). Unfortunately, we were unable to compute this minimum value because the computational cost became prohibitive at this close spacing. However, with runs taking N up to 12 and M up to 9, we were able to conclude that this minimum must occur in the range $2 \leqslant R/a \leqslant 2.02$.

Figure 12 shows the trajectories of a neutrally buoyant sphere of unit radius in a shear flow in the presence of a fixed sphere of equal size centered at the origin. The dashed line surrounding the fixed sphere represents the positions of the center of the neutrally buoyant sphere when its surface touches the fixed sphere. The curved dashed line indicates the positions of the sphere center where

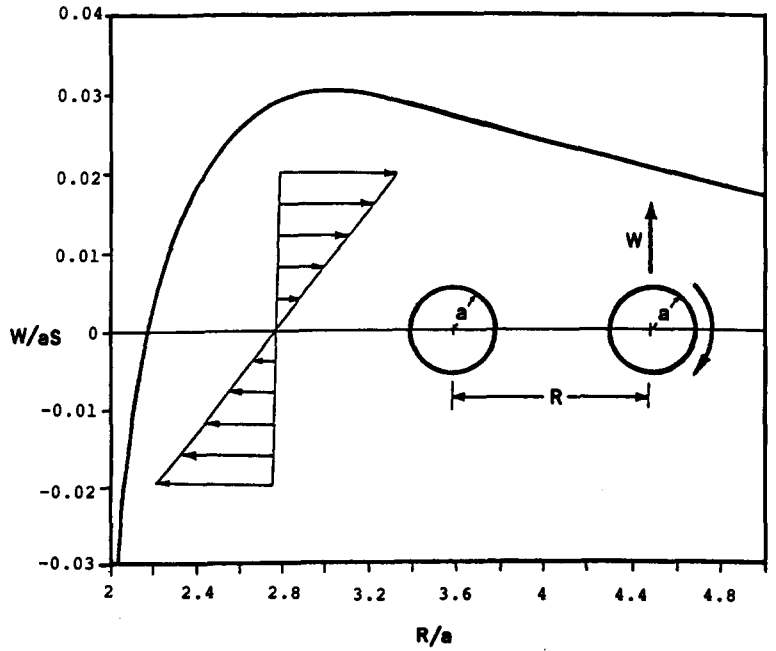

Figure 11. Translational velocity of the neutrally buoyant sphere.

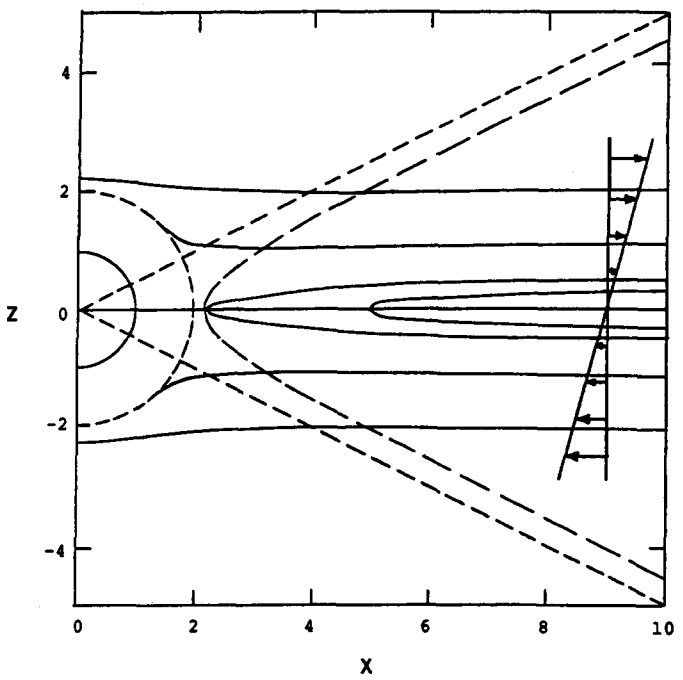

Figure 12. Trajectories of a neutrally buoyant sphere in the presence of a rigidly held sphere in shear flow.

the z-velocity component of the neutrally buoyant sphere vanishes, and thus represents the locus of minimum distance between the trajectories and the plane of symmetry $z = 0$. Also shown is the asymptotic value of this curve $z = \pm(1/2)x$ obtained by setting $w = 0$ in [18c]. For $x = 10$ and $-0.48 \leqslant z < 0$, the neutrally buoyant sphere approaches the fixed sphere but is swept up and away before ever reaching it in a mirror image trajectory about the plane $z = 0$. For $x = 10$ and $z < -0.48$, the neutrally buoyant sphere will approach the fixed sphere and swing around beneath it in a mirror image trajectory about the plane $x = 0$.

7. CONCLUDING REMARKS

The multipole truncation technique developed by Hassonjee *et al.* (1988) for treating the hydrodynamic interaction of arbitrary three-dimensional clusters of spherical particles has been applied to study the behavior of systems of particles in planar shear and Poiseuille flows. This method has the drawback of using large computer memory and computational time as mentioned previously (Hassonjee *et al.* 1988). Nevertheless, we have been able to do transient problems involving three particles accurately using the CRAY II and IBM 3090 supercomputers.

As demonstrated in the earlier sections, this is a powerful technique to study accurately the behavior of a finite number of particles in a viscous media. One may also easily and accurately determine the fluid behavior around a finite number of spheres, which should provide a better understanding of convective heat and mass transfer in suspensions. Although the method is time consuming when used for time-dependent problems involving more than three particles at close spacings, it serves to check the validity and accuracy of other faster but approximate methods, such as the multipole moment technique of Durlofsky *et al.* (1987). One can also compromise with the desired accuracy and is thus able to increase the number of particles considered. During the course of this study we have seen the development and use of larger and faster computers, and with this kind of progress we may be able to use this method for transient problems involving more than three particles in the near future. At this time, this method can also be modified to solve bounded flow problems accurately where only a small number of particles are involved.

Acknowledgements—The authors wish to thank the National Science Foundation for supporting this research under Creativity Grant CPE 85-00301. The authors gratefully acknowledge the NSF Office of Advanced Scientific Computing for providing access to the CRAY I and CRAY II supercomputer facilities at the University of Minnesota and the IBM 3090 parallel processing facilities at Cornell University. The authors also wish to thank Professor A. Nir of Technion—Israel Institute of Technology for his help and suggestions during his visit to CCNY and the reviewers for their useful comments and suggestions. The above work has been performed in partial fulfillment of the requirements for the Ph.D. Degree of Q. Hassonjee from The Graduate School of The City University of New York.

REFERENCES

ARP, P. A. & MASON, S. G. 1977 The kinetics of flowing dispersions. VIII. Doublets of rigid spheres (theoretical). *J. Colloid Interface Sci.* **61,** 21–43.

BRENNER, H. 1964 The Stokes resistance of an arbitrary particle—II. An extension. *Chem. Engng Sci.* **19,** 599–629.

BRENNER, H. & O'NEILL, M. E. 1972 On the Stokes resistance of multiparticle systems in a linear shear field. *Chem. Engng Sci.* **27,** 1421–1439.

DURLOFSKY, L. & BRADY, J. F. 1989 Dynamic simulation of bounded suspensions of hydrodynamically interacting particles. *J. Fluid Mech.* **200,** 39–67.

DURLOFSKY, L., BRADY, J. F. & BOSSIS, G. 1987 Dynamic simulation of hydrodynamically interacting particles. *J. Fluid Mech.* **180,** 21–49.

HAPPEL, J. & BRENNER, H. 1973 *Low Reynolds Number Hydrodynamics*, 2nd edn. Noordhoff, Leyden.

HASSONJEE, Q. 1987 An 'exact' solution for the hydrodynamic interaction of a three-dimensional finite cluster of arbitrarily sized spherical particles at low Reynolds number. Ph.D. Dissertation, The City Univ. of New York.

HASSONJEE, Q., GANATOS, P. & PFEFFER, R. 1988 A strong interaction theory for the motion of arbitrary three-dimensional clusters of spherical particles at low Reynolds number. *J. Fluid Mech.* **197,** 1–37.

KAMEL, M. T. & TORY, E. M. 1989 Sedimentation of clusters of identical spheres I. Comparison of methods for computing velocities. *Powder Technol.* **59,** 227–248.

KOCH, D. L. 1989 On hydrodynamic diffusion and drift in sheared suspensions. *Phys. Fluids.* **A1,** 1742–1745.

KYNCH, G. J. 1959 The slow motion of two or more spheres through a viscous fluid. *J. Fluid Mech.* **5,** 193–208.

LADD, A. J. C. 1988 Hydrodynamic interactions in a suspension of spherical particles. *J. Chem. Phys.* **88,** 5051–5063.

LEIGHTON, D. & ACRIVOS, A. 1987 The shear-induced migration of particles in concentrated suspensions. *J. Fluid Mech.* **181,** 415–439.

LIN, C. J., LEE, K. J. & SATHER, N. F. 1970 Slow motion of two spheres in a shear field. *J. Fluid Mech.* **43,** 35–47.

MAZUR, P. & VAN SAARLOOS, W. 1982 Many-sphere hydrodynamic interactions and mobilities in a suspension. *Physica* **115A,** 21–57.

TRAN-CONG, T. & PHAN-THIEN, N. 1989 Stokes problems of multiparticle systems: a numerical method for arbitrary flows. *Phys. Fluids* **A1,** 453–461.

APPENDIX

This appendix contains final expressions used to compute the unknown coefficients $A_{jmn} - F_{jmn}$ in [6] for J spheres in planar shear and/or Poiseuille flow. The results are:

for the r-component of velocity,

$$A'_0(\theta_k) = W_k \cos\theta_k - \frac{1}{2\pi}\int_0^{2\pi} \sum [A_{jmn}A'_{jkmn} + \cdots + F_{jmn}F'_{jkmn}]\,\mathrm{d}\phi_k, \qquad [A.1]$$

$$A'_1(\theta_k) = U_k \sin\theta_k - S(a_k\cos\theta_k + d_k)\sin\theta_k - \alpha\left[1 - \frac{(a_k\cos\theta_k + d_k - \eta)^2}{\beta^2}\right]\sin\theta_k$$
$$- \frac{1}{\pi}\int_0^{2\pi}\sum[A_{jmn}A'_{jkmn} + \cdots + F_{jmn}F'_{jkmn}]\cos\phi_k\,d\phi_k, \qquad [A.2]$$

$$B'_1(\theta_k) = V_k\sin\theta_k - \frac{1}{\pi}\int_0^{2\pi}\sum[A_{jmn}A'_{jkmn} + \cdots + F_{jmn}F'_{jkmn}]\sin\phi_k\,d\phi_k, \qquad [A.3]$$

$$\begin{Bmatrix}A'_{m'}(\theta_k)\\ B'_{m'}(\theta_k)\end{Bmatrix} = -\frac{1}{\pi}\int_0^{2\pi}\sum[A_{jmn}A'_{jkmn} + \cdots + F_{jmn}F'_{jkmn}]\begin{Bmatrix}\cos m'\phi_k\\ \sin m'\phi_k\end{Bmatrix}d\phi_k \quad m' > 1; \qquad [A.4]$$

for the θ-component of velocity,

$$A''_0(\theta_k) = -W_k\sin\theta_k - \frac{1}{2\pi}\int_0^{2\pi}\sum[A_{jmn}A'_{jkmn} + \cdots + F_{jmn}F''_{jkmn}]\,d\phi_k, \qquad [A.5]$$

$$A''_1(\theta_k) = a_k(\Omega_y)_k - \alpha\left[1 - \frac{(a_k\cos\theta_k + d_k - \eta)^2}{\beta^2}\right]\cos\theta_k - S(a_k\cos\theta_k + d_k)\cos\theta_k$$
$$+ U_k\cos\theta_k - \frac{1}{\pi}\int_0^{2\pi}\sum[A_{jmn}A''_{jkmn} + \cdots + F_{jmn}F''_{jkmn}]\cos\theta_k\,d\phi_k, \qquad [A.6]$$

$$B''_1(\theta_k) = V_k\cos\theta_k - a_k(\Omega_x)_k - \frac{1}{\pi}\int_0^{2\pi}\sum[A_{jmn}A''_{jkmn} + \cdots + F_{jmn}F''_{jkmn}]\sin\phi_k\,d\phi_k, \qquad [A.7]$$

$$\begin{Bmatrix}A''_{m'}(\theta_k)\\ B''_{m'}(\theta_k)\end{Bmatrix} = -\frac{1}{\pi}\int_0^{2\pi}\sum[A_{jmn}A''_{jkmn} + \cdots + F_{jmn}F''_{jkmn}]\begin{Bmatrix}\cos m'\phi_k\\ \sin m'\phi_k\end{Bmatrix}d\phi_k \quad m' > 1; \qquad [A.8]$$

and

for the φ-component of velocity,

$$A'''_0(\theta_k) = a_k(\Omega_z)_k\sin\theta_k - \frac{1}{2\pi}\int_0^{2\pi}\sum[A_{jmn}A'''_{jkmn} + \cdots + F_{jmn}F'''_{jkmn}]\,d\phi_k, \qquad [A.9]$$

$$A'''_1(\theta_k) = V_k - a_k(\Omega_x)_k\cos\theta_k - \frac{1}{\pi}\int_0^{2\pi}\sum[A_{jmn}A'''_{jkmn} + \cdots + F_{jmn}F'''_{jkmn}]\cos\phi_k\,d\phi_k, \qquad [A.10]$$

$$B'''_1(\theta_k) = -U_k - a_k(\Omega_y)_k\cos\theta_k + S(a_k\cos\theta_k + d_k) + \alpha\left[1 - \frac{(a_k\cos\theta_k + d_k - \eta)^2}{\beta^2}\right]$$
$$- \frac{1}{\pi}\int_0^{2\pi}\sum[A_{jmn}A'''_{jkmn} + \cdots + F_{jmn}F'''_{jkmn}]\sin\phi_k\,d\phi_k, \qquad [A.11]$$

$$\begin{Bmatrix}A'''_{m'}(\theta_k)\\ B'''_{m'}(\theta_k)\end{Bmatrix} = -\frac{1}{\pi}\int_0^{2\pi}\sum[A_{jmn}A'''_{jkmn} + \cdots + F_{jmn}F'''_{jkmn}]\begin{Bmatrix}\cos m'\phi_k\\ \sin m'\phi_k\end{Bmatrix}d\phi_k \quad m' > 1; \qquad [A.12]$$

where Σ denotes $\Sigma_{j=1(j\neq k)}^{J}\Sigma_{m=0}^{\infty}\Sigma_{n=m}^{\infty}$ and the functions $A'_0, \ldots, B'''_{m'}$ on the left-hand side of [A.1]–[A.12] are given in appendix C of Hassonjee *et al.* (1988) with m replaced by m'. The primed coefficients of the unknown constants on the right-hand side of [A.1]–[A.12] are given in appendix B of this same reference. Copies of these appendices may be obtained from the authors or the Editor on request.